ADAPTIVE CONTROL OF ROBOTS USING VISUAL FEEDBACK

L. E. Weiss, A. C. Sanderson and C. P. Neuman

The Robotics Institute, Carnegie-Mellon University, Pittsburgh, PA 15213, USA

Abstract

Vision-based robot control systems provide capabilities for modifying positions to accommodate uncertainty in the task environment. Vision-based robot control research has focused on vision processing issues, while control system design has been limited to ad-hoc strategies. In this paper, we formalize an analytical approach to the design of *dynamic* robot visual servo control systems. An image-based structure represents a new approach to visual servo control which uses local image features as feedback control signals. Image-based control presents formidable engineering problems for controller design, including complex dynamics, kinematics, and feature transformations, as well as unknown parameters, and measurement noise and delays. A model reference adaptive controller (MRAC) is designed to satisfy these requirements. Simulation studies are described which indicate the feasibility and expected performance of this approach for systems with 1, 2, and 3 degrees of freedom.

1. Introduction

Flexible robotic systems should provide capabilities to automatically modify positions, trajectories, and forces to accommodate uncertainty and change in a task or task environment. Visual sensing, in particular, provides fundamental capabilities for robot positioning tasks for both unstructured environments and precision applications. For example, visual feedback can be used to guide the to acquire unoriented objects, or used in the navigation of mobile robots. Another example is the use of visual information to automatically alter robot positions to accommodate parts tolerances and inaccurate modeling of robot arm and end-effector geometry in precision assembly operations. In these, as well as other sensor-based control applications, sensory measurements are used to derive feedback signals for robot control. The role of the sensor as the feedback transducer affects the closed-loop sensory control system dynamics, and a sensory feedback controller is required for stability and acceptable transient response. The problems encountered with the design of such systems include the interpretation of complex sensory signals, and synthesis of a control law which accounts for any nonlinear, unknown, and coupled properties of the sensor system, as well as those of the robot.

As a case study of sensory control, we have conducted extensive analysis, design, and mainframe simulation studies of dynamic visual servoing systems[1]. Vision-based robot control research has focused on vision processing issues (e.g., image filtering, structured lighting environments, and image feature interpretation), while control system design has been limited to mostly ad-hoc strategies. Our research formalizes an analytical approach to *dynamic* robot visual servo control systems by first organizing and categorizing visual control strategies into well-defined feedback control structures, which are classified into *position-based* (world coordinate frame) and *image-based* (sensor coordinate frame) structures. In the position-based approaches, the visual measurements must first be interpreted in terms of a robot joint or a world coordinate frame since robot task and trajectory planning are typically formulated in such frames. The the interpretation of two dimensional image information to estimate world positions normally requires the extraction of quantitative image features which are related to stored object and transducer models. The positional error signal, between reference and measured positions, may be used to design a "position-based" visual servo control system[2, 3, 4, 5, 6]. The image-based structure represents a new approach to visual servo control, in which the task is defined directly in terms of the sensor coordinate frame. In this approach, image features which are monotonically related to spatial position may be used as a basis for control in place of position estimates, thus eliminating a complex interpretation step. These features include quantitative parameters associated with the structural components of the two dimensional image such as points, lines, and connected regions. For example, typical features are centroids, angles, lengths, and areas. The feedback and reference signals are then defined in terms of these feature space measurements. Such an "image-based" visual servo control strategy may offer advantages in terms of reduced delay and estimation noise, and provide a convenient means for robot task training by using a "teach-by-showing" strategy for specification of the control system reference signal commands.

In the position-based control approaches, the vision system is used as a transducer to measure the relative positions $\underline{X}_{rel}$ between the robot end-effector and some object in it's environment. This measurement process can be decomposed into two nonlinear transformations. First, the transduction and feature extraction functions, or world-to-feature space transformation, can be viewed as the inverse of an ideal interpretation, in the absence of noise, according to:

$$\underline{f} = I^{-1}[\underline{X}_{rel}] \qquad (1)$$

where $\underline{f}$ are the features and I is "ideal" in the sense of being based on exact object and image transducer models. Second, the features are mapped to world space by the approximate interpretation transformation:

$$\hat{\underline{X}}_{rel} = \hat{I}[\underline{f}] \qquad (2)$$

where, modeling inaccuracies and image transducer noise lead to equivalent measurement noise. If the interpretation has a unique inverse mapping. over the control region of interest, such that $\underline{X}_{rel}$ are single-valued functions of $\underline{f}$, then this suggests that the system can be controlled, to unique end-points, using features directly as the feedback and reference signals, thus eliminating the interpretation step. The uniqueness condition is satisfied, for the control region of interest, when the first partial derivatives of $\underline{f}$ are continuous, and the Jacobian of the ideal inverse interpretation is nonsingular; i.e.,

*This work has been supported in part by the Westinghouse Electric Corporation and in part by the Robotics Institute of Carnegie-Mellon University

$$\det \frac{\partial l^{-1}[\underline{X}_{rel}]}{\partial \underline{X}_{rel}} \doteq \det[J_{feat}] \neq 0 \qquad (3)$$

where J_{feat} is defined as the feature sensitivity matrix. In practice, J_{feat} could be estimated on-line to test the condition in equation (3). This condition must be true for both position and image-based approaches. Further, since the determinant is only defined for square matrices, then the permitted number of degrees-of-freedom must equal the number of measured features.

A digitally controlled image-based visual servo (IBVS) control structure, which uses feature feedback, is represented in Figure 1-1. This system was first first proposed by Sanderson and Weiss[7]. In Figure 1-1, $\underline{u}$ are the control signals, $\underline{q}$ are the robot joint coordinates, and n_d is the number of feedback delays introduced by the vision processing. The characteristics of each block are described in the next section. The reference feature signal $\underline{f}_{ref}(k)$ can be defined using a "teach-by showing" strategy whereby an image is transduced in the desired reference position and the corresponding extracted features represent the reference feature values. To further simplify the task training requirements, we have assumed that in the "teach-by-showing" approach, the inverse transformation l^{-1} is unknown. Therefore, the controller C must be based on a design approach which not only compensates for the nonlinear and coupled properties of l^{-1}, but also for unknown values.

2. Adaptive Control of Image-Based Systems

To design a controller, it is useful to first consider the small-signal model (about a nominal operating point or trajectory) of an the IBVS structure in Figure 1-1. The control signals are applied through digital-to-analog converters (DAC) which can be modeled by the cascade of an ideal impulse sampler and a zero-order hold with a saturation nonlinearity. The system output is the undelayed feature, while the feedback path is modeled by discrete unit delays. Linearized open-loop robot dynamics[8], or equivalent linear I/O models[9], are represented by the discrete-time Z-transformation $W_p(z^{-1})$. The feedback path is characterized by an overall small-signal sensitivity matrix J given by

$$J \doteq J_{feat}\, J_{arm} \qquad (4)$$

where J_{arm} is the arm Jacobian. In addition to the control requirements of the robot dynamics the design of the controller C also depends on the "J" sensitivity matrices, feedback delays, and measurement noise. The sensitivity matrices are nonlinear and coupled functions of $\underline{q}$ and $\underline{X}_{rel}$; thus, J varies as $\underline{q}$ varies, and feature-space transformations are manifested by time-varying open-loop gains. Predicted values of J can deviate from actual values due to inaccuracies in the modeling of the three dimensional object and transduction process, and from drift and variation in the transducer parameters. At the extreme, the values may be completely unknown a priori when minimal knowledge of the inverse interpretation transformations l^{-1} are available, such as arises when task programing is limited to the "teach-by-showing" strategy. A fixed controller design for these systems is a formidable engineering problem. An adaptive approach to controller design appears to be applicable for these requirements, and the IBVS controller design used in our research therefore emphasizes this approach.

The mathematical basis for our adaptive controller follows the enhanced identification error model reference adaptive control (MRAC) developed by Morris and Neuman[10]. Since the algorithm did not include control of systems with discrete measurement delays, we have extended it to include control of systems with delay[1].

Both single-input single-output (SISO) and multiple-input multiple-output (MIMO) equivalent model formulations can be used to derive the adaptive controller. In the context of joint-level robot control, Neuman and Stone[9] have justified the latter modeling approach by demonstrating that individual joints of a coupled and nonlinear robot can be modeled by linear time-varying second-order SISO transfer functions. While coupled, or MIMO, controllers have an inherently greater potential for being able to uncouple a coupled system they have several potential disadvantages, including computational complexity and they do not lend themselves to modularity. A modular system can easily be extended to increasing degrees-of-freedom, and distributed processing, and would thus be easier to implement in current laboratory and factory computing environments. For these reasons, the approach which we developed emphasized uncoupled control of coupled systems, using the concept of equivalent SISO plants. For example, a two degree-of-freedom (DOF) IBVS system is controlled by independent MRAC controllers in Figure 2-1.

An SISO MRAC for a system with n_d unit feedback delays is summarized here. In our approach, we assume that the variable under control is the measurable, or delayed, feature signal $f_d(k)$. An m^{th} order series-parallel reference model is described by the difference equation:

$$X^R_{SP}(k) = \Big[\sum_{i=1}^{m} b_i^{\circ} q^{-(i-1)}\Big] f_{Ref}(k) + \Big[\sum_{i=1}^{m} a_i^{\circ} q^{-(i-1)}\Big] f_d(k) \qquad (5)$$

In our studies we use second order models (i.e. m = 2) with the model parameters selected to achieve critical damping. The two reference model poles, located at $z = e^{-\omega_n T}$, specify the desired closed-loop bandwidth, ω_n, of the system. The maximum bandwidth is constrained by the sampling period, T, by

$$\frac{f_s}{f_{BW}} = \frac{1/T}{\omega_n/2\pi} = 2 \cdot PM. \qquad (6)$$

where a constant performance margin (PM) factor is included to reduce the specified bandwidth so that the identifier can track the time-varying parameters.

We assume that system under control can be modeled by the n^{th} order linear input/output equation

$$f_d(k) = \underline{\beta}^T \underline{\Phi}(k\text{-}1) \qquad (7)$$

where the (2n X 1) information vector is

$$\underline{\Phi}_d(k\text{-}1) \doteq [u(k\text{-}1\text{-}n_d) \ldots u(k\text{-}n\text{-}n_d)\; f_d(k\text{-}1) \ldots f_d(k\text{-}n_d)]^T$$

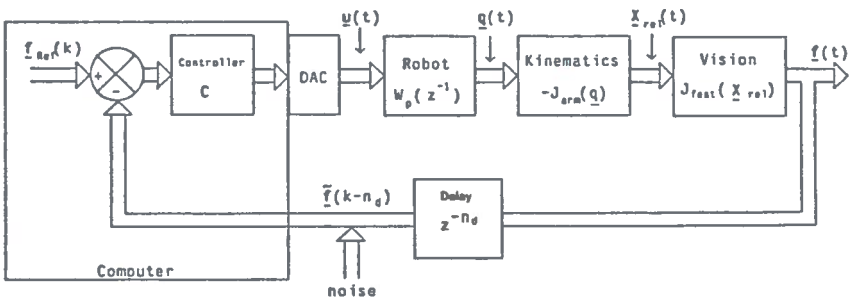

Figure 1-1: Image-Based Visual Servoing

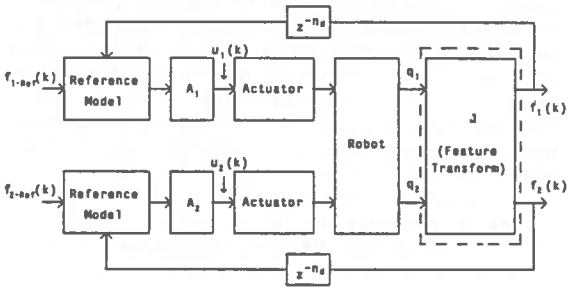

Figure 2-1: MRAC Control of an IBVS System

and the (2n X 1) parameter vector is

$$\underline{\beta}^T \doteq (b_1 \ldots b_n a_1 \ldots a_n) \tag{8}$$

A series-parallel identifier predicts the delayed feature signal by

$$\underline{\hat{t}}_d(k) = \hat{\underline{\beta}}^T(k\text{-}1\text{-}n_d)\underline{\Phi}_d(k\text{-}1) \tag{9}$$

where $\hat{\underline{\beta}}$ is the estimated parameter vector. The identification error is

$$e_{ID}(k) = f_d(k) - t_d(k)$$

A hyperstable adjustment mechanism specifies the following identifier when the plant is assumed to be linear with slowly varying parameters:

$$\hat{\underline{\beta}}(k\text{-}n_d) = \hat{\underline{\beta}}(k\text{-}1\text{-}n_d) + \frac{1}{\lambda}P(k\text{-}1)\underline{\Phi}_d(k\text{-}1)s(k) \tag{10}$$

$$s(k) = \frac{e_{ID}(k)}{1 + (1/\lambda)\underline{\Phi}^T{}_d(k\text{-}1)P(k\text{-}1)\underline{\Phi}_d(k\text{-}1)} \tag{11}$$

$$P(k) = \frac{1}{\lambda}P(k\text{-}1) - \frac{1}{\lambda^2}\frac{s(k)}{e_{ID}(k)}P(k\text{-}1)\underline{\Phi}_d(k\text{-}1)\underline{\Phi}^T{}_d(k\text{-}1)P(k\text{-}1) \tag{12}$$

where P(k) is a (2n X 2n) adaptive gain matrix, s(k) is the a'posteriori error, e_{ID} is the a'priori error signal, and the fading factor λ ($0<\lambda\leq 1$) weighs past values of the input/output samples. The controller is derived by solving (9) for the control signal u(k) required to force the one-step ahead identifier output $t_d(k+1)$ to follow the reference signal $X^R(k)$. We do not use a predictor to estimate the actual, or undelayed, feature signal. Using this approach we can at best calculate what the control signal $u(k\text{-}n_d)$ should have been n_d sampling instants in the past, and force the result to be u(k). Inverting (9) for $u(k\text{-}n_d)$, and and forcing the control signal to this value, we obtain:

$$u(k) = \frac{1}{\hat{b}_1(k\text{-}n_d)}\left\{X^R_{SP}(k) - \left[\sum_{i=2}^{n}\hat{b}_i(k\text{-}1\text{-}n_d)q^{-(i-1+n_d)}\right]u(k) - \left[\sum_{i=1}^{n}\hat{a}_i(k\text{-}1\text{-}n_d)q^{-(i-1)}\right]y_d(k)\right\} \tag{13}$$

A control penalty must be applied to (13) to insure a stable and bounded control signal. A control signal penalty is obtained by multiplying (13) by the positive scaler $\pi(k)$ ($0<\pi\leq 1$). The penalty also reduces the effects of control signal saturation, noise, and under estimation of b_1. To derive the control penalty, the Jury stability conditions are applied to test the location of the controller poles at each computational cycle. When pole magnitudes exceed the design parameter γ, where $0<\gamma<1$, the value of π is reduced until the poles lie within a circle of radius γ in the Z-plane. In our studies we used second order identifiers and assumed a single measurement delay (i.e., $n_d = 1$), thus the control penalty is computed as

$$\pi(k) = \begin{cases} 1 \quad \text{for} \quad |\hat{b}_2/\hat{b}_1| < \gamma^2 \\ [\hat{b}_1(k)/\hat{b}_2(k)]\gamma^2 \quad \text{for } |\hat{b}_2/\hat{b}_1| > \gamma^2 \end{cases} \tag{14}$$

2.1. Feature Assignment Using Diagonal Dominance

The feature assignment process asks: Since uncoupled controllers are used to control coupled plants, then for a set of of n outputs f_i ($i = 1,\ldots,n$), which servo error, Δf_i, should be filtered and coupled to the j^{th} joint actuator as u_j? We have developed a measure of system coupling to help answer this question. To formalize this procedure let an open-loop linear system be defined by

$$\underline{f}(s) = H(s)\underline{u}(s) \tag{15}$$

where H(s) is an (n x n) transfer function matrix. If the system is uncoupled, H(s) can be transformed into a diagonal matrix by switching the j^{th} and k^{th} columns of H(s), and therefore the j^{th} and k^{th} rows of $\underline{u}(s)$, until all off diagonal elements of H(s) are zero. When H(s) is diagonal, the only choice for servo error/actuator assignment is $u_i \leftarrow \Delta f_i$. When the system is coupled, then H(s) cannot be transformed into a diagonal matrix. Servo error/actuator assignment selection could be accomplished by organizing H(s) in a "diagonally dominant" fashion[11], such that the diagonal elements dominate the off-diagonal elements. Diagonal dominance is defined as

$$|H_{ii}(s)| > \sum_{\substack{j=1 \\ j\neq i}}^{n} |H_{ij}(s)| \quad \text{for } i = 1,\ldots n \tag{16}$$

However, when applied to image-based systems, with $JW_p \leftarrow H(s)$, we have shown that the sensitivity matrices cannot in general satisfy this definition of dominance. An alternative approach is to organize JW_p to maximize the inequality (16) over all possible column arrangements. This criterion reduces to defining the dimensionless measure of diagonal dominance as

$$D(k) = \log \sum_{\substack{i=1 \\ j\neq i}}^{n} \sum_{j=1}^{n} \frac{|JW_{p\text{-}ij}(k)|}{|JW_{p\text{-}ii}(k)|} \tag{17}$$

and then minimizing $D(JW_p)$ over all n! possible column arrangements. The logarithm of the dominance is used since the ratios change by orders of magnitude. Our evaluation shows that control system performance improves as features are selected and assigned according to (17).

2.2. Feature Selection

The image of a typical scene generally contains more features than there are degrees-of-freedom to control. The number of features must equal the number of degrees-of-freedom in an image based system since the feature sensitivity matrix is constrained to be square. The feature selection process asks the question: How should a subset of n features be selected from a set of m possible control features f_i ($i = 1,\ldots,m$), where m>n? The possible number of ordered candidate feature subsets is

$$p(m,n) = \frac{m!}{(m\text{-}n)!} \tag{18}$$

where ordering is required to consider the feature/joint assignment.

To arrive at a criterion for feature selection, two aspects of feature-based control are analyzed:

1. Ability to specify world space path using feature based trajectories (assuming that the control system can achieve a specified feature space performance), and

2. The control effort required to achieve the specified feature space dynamic performance.

It is shown below that the attributes of the feature sensitivity matrix, J_{feat}, relate to path performance, while the attributes of JW_p relate to the control effort aspects.

With respect to world space path, it is desirable to be able to control independently each world level DOF. To achieve this goal, an ideal subset of features should yield a feature sensitivity J_{feat} which is diagonal and constant. If an ideal feature sensitivity matrix could be synthesized, then it still remains to control dynamically the system to achieve the desired feature response. Attributes of the overall sensitivity, JW_p, can be used to describe the control effort required to achieve the desired response. Similar to the feature sensitivity attributes, the idealized overall sensitivity matrix should be diagonal and constant. Diagonalization permits the unqualified use of independent SISO controllers. In our experience, these idealized sensitivity attributes cannot be expected in practice. The degrees-of-freedom are coupled and the sensitivities typically vary with position. Feature sensitivity changes are minimized for small motion tasks, and for configurations with large camera lens magnifications. However, if the feature sensitivity were constant, but coupled, the predicted path would be straight-line motion irrespective of the number of degrees-of-freedom. Since

$$\Delta \underline{X} = J_{feat}^{-1} \Delta \underline{f} \tag{19}$$

then

$$\Delta X_i = (J^{-1}_{feat\text{-}i,1}\Delta f_1 + \ldots + J^{-1}_{feat\text{-}i,n}\Delta f_n)(1-e^{-t/\tau})$$

$$= K_i(1-e^{-t/\tau}) \tag{20}$$

where, ΔX_i is the positional error for the i^{th} DOF, Δf_i is the i^{th} feature error, and $J_{feat\text{-}i,i}$ is the $(i,i)^{th}$ element of J_{feat}, and K_i is a constant. The constant relationship between any two Cartesian DOF becomes

$$\Delta X_i/\Delta X_j = K_i/K_j \tag{21}$$

which is the equation of a straight line.

Since we may not expect to find feature subsets which yield idealized sensitivity attributes, a feature selection strategy could seek a subset which best approximates these ideals; i.e., select features which minimize the coupling and sensitivity changes along a trajectory. In our research, the diagonal dominance measure, $D(JW_p)$, in (17), is used to quantify system coupling. The feature selection strategy then becomes minimizing $D(JW_p)$ and $D(J_{feat})$ over the set of candidate features. By minimizing $D(JW_p)$, improved dynamic response is achieved with SISO controllers. And, by minimizing $D(J_{feat})$, closer to monotonic path performance may be expected. Each strategy may not produce mutually exclusive decisions, and arbitration between them would be based on the relative importance of each attribute. For example, a system could be feature uncoupled in the joint space of an articulated robot arm, but not uncoupled in Cartesian space. Since the degree-of-coupling plays such an important role in the independent control approach, our initial research has focused on evaluation of feature selection based on minimization of $D(JW_p)$.

3. Simulation Studies

Adaptive IBVS systems are highly nonlinear, making it difficult to analytically predict their potential performance. Mainframe simulation studies were therefore used to evaluate IBVS control. The systems were modeled with progressively complex dynamics, kinematics, and feature coupling to understand their relative contributions to the control problem and system performance. Extensive studies have been completed for one, two and three DOF systems, and preliminary results are available for a 5 DOF system. Performance limitations and application of fixed controllers were also evaluated using linear model following controllers. Each LMFC is derived by fixing the gains of the adaptive controller to values derived from initial learning trials in the simulation experiments.

In these studies, the response to step-input reference signals, defined by the "teach-by-showing" strategy, provides a suitable measure of system performance. The reference model bandwidths were selected so that the sampling-to-bandwidth ratio f_s/f_{BW} was at least 20. To simplify the feature selection/assignment process, the low-frequency, or DC gain of W_p is used to calculate the coupling index D in equation (17). We observed that for a set of features, the feature/joint assignment remains constant over large regions of control for uncoupled kinematic configurations such as a Cartesian robot. For these configurations, off-line measurement of J in the initial image can be used to select a fixed assignment over the entire control trajectory. Off-line measurement to approximate J is accomplished by sequentially moving each robot joint by small increments, and measuring the accompanying change in features. For coupled kinematic configurations, such an articulated arm, a feature/joint reassignment is predicted when controlling over large distances in space, and a fixed feature/joint assignment is only suitable for applications requiring small corrective motions. Feature selection can also be based on initial image coupling if the potential candidates have relatively small coupling values.

The imaging camera is modeled as a pinhole lens, and image features are derived from the idealized non-distorted two-dimensional image points. Image distortions are difficult to model and vary widely with lighting, transducer resolution and linearity. These conditions are manifested as measurement noise and modeled using varying levels of uniformly distributed noise added to the idealized extracted feature values. Some representative examples of adaptive IBVS control are discussed below.

A single DOF study incorporates a camera which moves relative to a fixed line (or edge) in space. The camera is mounted to a dynamically linear translational stage, so that it is constrained to approach the line along a straight path. The control feature is the perceived line length. The feature sensitivity, over an 18 inch excursion, is displayed in Figure 3-1. The task is to move the camera from various initial starting positions to a desired position which is one inch from the line. The final or desired position of the camera was specified to be in close proximity to the line to accentuate rapidly changing feature sensitivities as the camera approaches the object. The sampling period is selected to be T = .033 seconds. In practice, if the visual system processing requires relatively long sampling periods, then higher sampling rate minor-loop velocity feedback controllers would be required to compensate for Coulomb friction, structural resonances, and to eliminate any apparent complex plane poles to satisfy the identifier's Nyquist sampling constraints. The fixed versus adaptive performance, as measured by position rise-time, is also displayed in Figure 3-1. While adaptive control performance remains constant over a wide range of excursions, fixed control response becomes sluggish. While adaptive control is superior for large motions, we also show that fixed controller performance improves at higher bandwidths, exhibits superior noise performance, and superior stability at lower sampling-to-bandwidth ratios.

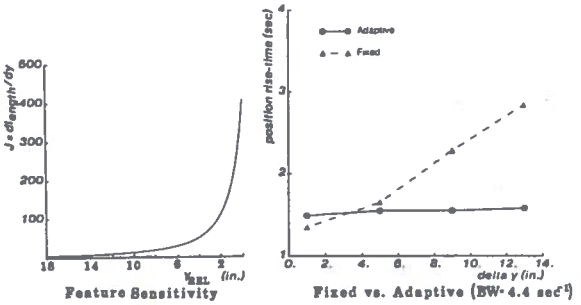

Figure 3-1: Single DOF Study

Another simulation included a dynamically nonlinear two DOF revolute joint articulated arm with a camera mounted to the second link. The task is to move the camera relative to a fixed line in space. For this task, there are two independent control features: the perceived centroid and line length. The coupling index is used to resolve the feature/joint assignment. Ranges of task motions included examples with initial to desired position trajectories of short excursions (e.g. one inch), to long range motions over two feet, and over a broad range of arm configurations. The dynamic robot model included Coriolis, centrifugal, viscous friction, and amplifier saturation. The sample period was T = .003 seconds. An example is shown in Figure 3-2 which displays the position trajectory of the camera and the corresponding rise-times. In Figure 3-2, the predicted trajectory is the path which would be achieved for perfect reference model following. The actual trajectory deviates from the predicted path due to initial transient identification errors which cannot be overcome in SISO control of the feature coupled system. The predicted trajectory deviates from a straight line by only .05 inches. For larger motion tasks, we observed that deviations of the predicted paths from a straight line remain on the same order of magnitude, even though the feature sensitivities are tightly coupled and vary dramatically over the trajectory. Actual path deviations from the predicted trajectories were acceptable for the larger motion tasks using a robot with linear uncoupled kinematics (e.g. X-Y translational stages) under adaptive control. However, with fixed controllers there were large path deviations and it was difficult to keep the line in the field of view. Using an articulated arm, for tasks requiring larger motions, the additional kinematic coupling leads to unacceptably large path deviations using either adaptive or fixed SISO controllers. These systems would require a coupled controller.

A three DOF configuration simulation consists of a stationary camera observing an object which is being moved. The object sits on top of a set of X-Y-θ translational and rotary stages. The task is to move the object relative to the fixed camera position. The extracted features available for polyhedral objects (e.g. cubes, pyramids, wedges, etc.) include the centroid and area of each visible plane, and the relative areas between any two adjacent planes. For this configuration there are more features available than there are degrees-of-freedom to control, and the coupling index is used to resolve both the feature selection and assignment. One method to evaluate the suitability of minimizing the coupling index to select features is to choose a very small motion task such that J, and thus $D(JW_p)$ stay essentially constant over the trajectory. System performance is evaluated for each possible combination of three features. For constant sensitivity, the X-Y stage predicted path is a straight line, and path performance is measured as the deviation from a straight line. Dynamic performance is evaluated as the position rise-time. For example, Figure 3-3 shows the path and rotation responses for three candidate features subsets when a cube is used as the object. Exhaustive testing shows that both path and dynamic performance improve as the coupling index decreases. For large motion tasks (e.g. trajectory greater than one foot), the observed paths approach straight lines as features are selected which reduce system coupling.

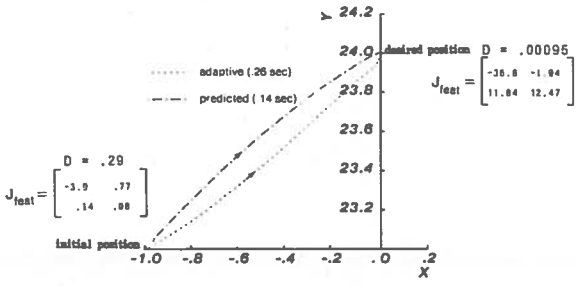

Figure 3-2: 2 DOF TASK

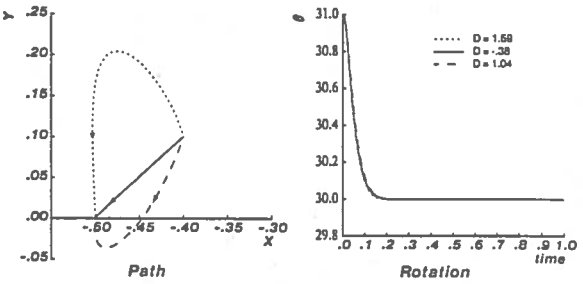

Figure 3-3: 3 DOF Examples

4. Conclusion

In this paper we develop a strategy for defining robot visual servoing tasks, and thus control, directly in the sensor coordinate frame. The role of adaptive control as a means to achieve consistent dynamic response in such systems is identified and evaluated. Analysis and simulation of the adaptive image-based visual servo control (IBVS) approach suggests that implementations of such systems may provide speed, accuracy, and simplified task training relative to position-based approaches. While image-based control does not provide for explicit specification of the position trajectories, we have shown that smooth trajectories which approximate straight line motion can be achieved. In this sense, IBVS provides for an inherent strategy for adaptive trajectory planning. For regimes of movement where image features have well-defined relations to the task, IBVS provides a useful complement to position-based control. In mobile robot navigation this complementary IBVS/position-based approach might be useful as a basis for control with respect to navigation features in an unstructured environment.

References

1. Weiss, Lee E., *Dynamic Visual Servo Control of Robots: An Adaptive Image-Based Approach*. PhD dissertation, Carnegie-Mellon University, 1984.
2. Sanderson, A. C., Weiss, L., "Adaptive Visual Servo Control of Robots", in *Robot Vision*, Pugh, A., ed., I.F.S. Publications Ltd., International Trends In Manufacturing Technology, 1983.
3. Agin, G.J., "Real Time Control of a Robot with a Mobile Camera", Tech. report 179, SRI International, Feb. 1979.
4. Geschke, C., "A Robot Task Using Visual Tracking", *Robotics Today*, Winter 1981-1982, pp. 39-43.
5. Albus, J. S., et al., "Hierarchical Control for Sensory Interactive Robots", *11th International Symposium on Industrial Robots*, SME and RIA, Oct. 1981, pp. 497-505.
6. Ward, M. R., et al., "Consight: A Practical Vision-Based Robot Guidance System", *9th International Symposium on Industrial Robots*, SME and RIA, March 1979, pp. 195-211.
7. Arthur C. Sanderson and Lee E. Weiss, "Image-Based Visual Servo Control of Robots", *26th Annual SPIE Technical Symposium*, SPIE, August 1982.
8. Chung, M.J., and Lee, C.S.G., "An adaptive Control Strategy for Computer-Based Manipulators", Tech. report 10-82, The Univ. of Michigan, Ann Arbor, August 1982.
9. Stone, H. and Neuman, C.P., "Dynamic Modeling and Adaptive Control of a Three DOF Robotic Manipulator", *IEEE Transactions on Systems, Man, and Cybernetics*, Vol. 14, July 1984.
10. Neuman, C.P. and Morris, R.L., "Classical Control Interpretation and Design of Microcomputer Adaptive Controllers", in *Applications of Adaptive Control*, Academic Press, 1980.
11. Rosenbrock, H. H., *Computer-Aided Control System Design*, Academic Press, 1974.